Energy Conversion and Management 254 (2022) 115268

Contents lists available at ScienceDirect

Energy Conversion and Management

journal homepage: www.elsevier.com/locate/enconman

Regional supply chains for decarbonising steel: Energy efficiency and green premium mitigation

Alexandra Devlin, Aidong Yang *

Department of Engineering Science, University of Oxford, Parks Road, Oxford OX1 3PJ, United Kingdom

ARTICLE INFO

Keywords:
Decarbonised steel
Green hydrogen
Regional alliances
Supply chains
Energy efficiency
Green premium

ABSTRACT

Decarbonised steel, enabled by green hydrogen-based iron ore reduction and renewable electricity-based steel making, will disrupt the traditional supply chain. Focusing on the energetic and techno-economic assessment of potential green supply chains, this study investigates the direct reduced iron-electric arc furnace production route enabled by renewable energy and deployed in regional settings. The hypothesis, that co-locating manufacturing processes with renewable energy resources would offer highest energy efficiency and cost reduction, is tested through an Australia-Japan case study. The binational partnership is structured to meet Japanese steel demand (for domestic use and regional exports) and source both energy and iron ore from the Pilbara region of Western Australia. A total of 12 unique supply chains differentiated by spatial configuration, timeline and energy carrier were simulated, which validated the hypothesis: direct energy and ore exports to remote steel producers (i.e. Japan-based production), as opposed to co-locating iron and steel production with abundant ore and renewable energy resources (i.e. Australia-based production), increased energy consumption and the levelised cost of steel by 45% and 32%, respectively, when averaged across 2030 and 2050. Two decades of technological development and economies of scale realisation would be crucial; 2030 supply chains were on average 12% more energy-intense and 23% more expensive than 2050 equivalents. On energy vectors, liquefied hydrogen was more efficient than ammonia for export-dominant supply chains due to the pairing of its process flexibility and the intermittent solar energy profile, as well as the avoidance of the need for ammonia cracking prior to direct reduction. To mitigate the green premium, a carbon tax in the range of A$66–192/t CO_2 would be required in 2030 and A$0–70/t CO_2 in 2050; the diminished carbon tax requirement in the latter is achievable only by wholly Australia-based production. Further, the modelled system scale was immense; producing 40 Mtpa of decarbonised steel will require 74–129% of Australia's current electricity output and A$137–328 billion in capital investment for solar power, production, and shipping vessel infrastructure. These results call for strategic planning of regional resource pairing to drive energy and cost efficiencies which accelerate the global decarbonisation of steel.

1. Introduction

Steel production is one of the world's most energy-intensive sectors with an annual production of 1.9 billion tonnes and energy consumption of 845 Mtoe, equivalent to 20% of global industrial energy use [29,68]. Persistent reliance on carbon-intensive steel production is undermining global efforts to reach net zero emissions of greenhouse gases (GHG). The iron and steel sector constitutes 7% (2.6 Gt CO_2/yr) of global energy-related GHG emissions [29]. The pressure to decarbonise is immense, derived from global and national bodies, financiers, and downstream end-use sectors [57]. Acknowledging this, 50% of major steel companies have pledged net zero-carbon emissions by 2050 [30].

The high level of energy consumption and GHG emissions of steel production is largely driven by the primary blast furnace-basic oxygen

Abbreviations: AU, Australia; BF, blast furnace; BOF, basic oxygen furnace; BOG, boil-off gas; CAPEX, capital expenditure; CGH_2, compressed gaseous hydrogen; CO_2, carbon dioxide; DRI, direct reduction of iron; EAF, electric arc furnace; FC, fuel cell; HBI, hot briquetted iron; H_2, hydrogen; JP, Japan; LCOE, levelised cost of electricity; LCOS, levelised cost of steel; LH_2, liquid hydrogen; LS, liquid steel; NH_3, ammonia; NPV, net present value; OPEX, operational expenditure; PEMFC, proton exchange membrane fuel cell; SC, supply chain; SI, supplementary information; SOFC, solid oxide fuel cell; VRE, variable renewable energy; VRE_{on}, daylight hours; VRE_{off}, non-daylight hours.

* Corresponding author.
E-mail address: aidong.yang@eng.ox.ac.uk (A. Yang).

https://doi.org/10.1016/j.enconman.2022.115268
Received 20 October 2021; Received in revised form 10 January 2022; Accepted 17 January 2022
Available online 26 January 2022

furnace (BF-BOF) route which uses carbon as the iron ore reductant and accounts for approximately 70% of global production [68]. Secondary steel produced using recycled steel in the electric arc furnace (EAF) accounts for another 25%, though production is understandably constrained by scrap supply. In the context of a growing need for new stocks in developing economies, secondary steel has been predicted to be able to meet only 55% of construction-related steel demand globally by 2050 [13]. Reliance on secondary steel is also compromised by copper contamination. Although manageable by trade and dilution to match end-use with steel quality, this strategy will become increasingly difficult towards 2050 [11]. Hence, fossil-free primary steel production needs to be commercialised well before 2050 to minimise industry's contribution to the global carbon budget.

Directly reducing iron (DRI) followed by refinement in an electric arc furnace (EAF) is an alternative primary production process that accounts for 5% of total steel production and presents an opportunistic platform for decarbonisation [17]. Although the iron ore reductant is currently syngas (mixture of carbon monoxide and hydrogen (H_2) produced using natural gas or coal), switching to 100% H_2 will mitigate CO_2 emissions in the DRI shaft furnace. If both water electrolysis for H_2 production and the EAF are powered by renewable energy, CO_2-free steel is enabled. Recent techno-economic assessments of the H_2-DRI-EAF process have validated the process efficacy: quantifying specific energy consumption at process-level [63], assessing heat integration efficiency gains [34] and optimising process flexibility [42]. This novel process is now being piloted by steel industry leaders including SSAB and ArcelorMittal [41]. It is acknowledged that syngas may also be substituted by a biomass oxy-fuel furnace to facilitate decarbonised steel production via direct reduction [4], however the allocation of biomass resources presents supply chain uncertainty [53].

In addition to technology migration, the globalised trade of steel means that the geography of resources and the decarbonisation of the sector are closely linked. Supply chain relocation associated with the steel production paradigm shift to net zero is an emerging area of research. Of particular interest is the binational partnership between Australia (AU), a mineral and energy exporter, and Japan (JP), a steel product user and exporter. Relevant trade links are already established between the two nations; Japan's imports of Australian iron ore represent 4% of global ore trade (8% Japanese share of Australia's exports which is 53% of global trade) [15]. Japan is the second largest global steel exporter after China [68], serving Asia's developing economies. Moreover, both nations are actively promoting a hydrogen-based economy and collaborating on the Hydrogen Energy Supply Chain Project, a world-first initiative which aims to produce and transport blue hydrogen from Latrobe Valley, Australia, to Kobe, Japan [10]. Therefore, this study utilises the Australia-Japan partnership as a case study for global clean energy-driven manufacturing.

Systems integration research which investigates cost-effective and reliable means of energy provision is necessary to enable decarbonisation solutions [12]. Considering Australia and its East Asian regional links, Gielen et al. [21] discussed the strategy of large-scale DRI production in Australia using local renewable energy, and exporting DRI as opposed to iron ore. The Grattan Institute [67] investigated the H_2-DRI-EAF supply chain in this region and estimated the levelised steel production cost of three pathways with Australia exporting green steel, DRI and iron ore (with hydrogen), respectively. While both studies are inspirational, what remains to be explored is a detailed assessment of energy utilisation efficiency of different supply chain configurations and a corresponding techno-economic analysis within the projected decarbonisation timeline. The energetics of fossil-free steel production systems, recently assessed in the UK based on 7 Mt of domestic production [47], remains under-researched for other regional settings. Steel, like many other hard-to-abate sectors, pertains a decarbonisation pathway that depends on an affordable, readily available, fossil-free energy system and effective supply-and-demand balancing mechanisms to manage the coupling of intermittent renewable energy and inflexible industrial processes. Effective energy planning for fossil-free steel systems is yet to be explored in-depth.

This study addresses the aforementioned literature gap and attempts to answer the question of how different supply chain configurations would affect the technical and economic performance of a regional green steel initiative. More specifically, this work tests the hypothesis that co-locating high-quality renewable energy resources, iron ore reserves, and manufacturing facilities will drive energy- and cost-efficiency through a comprehensive energetic and techno-economic assessment of the Australia-Japan link for green steel. Zero carbon H_2-DRI-EAF supply chain configurations are established for representative time periods (i.e. 2030 and 2050) and vary in the spatial locations of DRI and EAF, each encompassing renewable energy supply, iron and steel production and shipping. While the assessed options are similar to the "pathways" considered by Wood et al. [67], they are investigated here with detailed modelling of the processes of energy production and storage, steel production, and transport, to derive energy efficiency and costs, which is necessary for enabling comprehensive and transparent comparisons between different options. Furthermore, the assessment has considered two different H_2 energy vectors (liquified hydrogen and ammonia); to the authors' knowledge, this is the first comparative study of the two energy vectors within the context of complete green steel supply chain. Such understanding is important for revealing key factors affecting the performance at the entire supply chain level, hence providing valuable guidance to future decision making in technical, business and policy development.

This work aims to reveal how different designs of the Australia-Japan regional link affect (1) the overall energy efficiency, and (2) the economic competitiveness of fossil-free steel in light of the acknowledgement of the financial burden of the technological solution as a major challenge of steel decarbonisation [17]. Quantification of green premiums (the additional cost of fossil-free alternatives) enables establishment of baseline market competitiveness, and determination of carbon prices which have been proven influential in incentivising industrial emitters to enhance energy efficiency and invest in renewables [70]. The positive correlation between manufacturing efficiency, economic competitiveness, and carbon emission reductions which has been investigated in the Australian context [71] is further explored in this study. The adoption of a systems perspective and binational case study is intended to deliver results relevant to industrial change on a global stage.

2. Methods

In this section, the system definition and cases covered by this study are first introduced, followed by a technical description of the four major decarbonised steel production capabilities: (i) renewable energy supply, (ii) iron and steel production, (iii) H_2 production, storage and conversion, and (iv) shipping. Approaches to energy and economic assessments are also established. For each case, the energy assessment quantifies total energy consumption per tonne of steel product and derives pathway energy efficiency (from renewable energy supply to end use) of key subsystems. On the economic side, levelised cost of steel is the key metric quantified, together with the levelised cost of energy and that of hydrogen production. In general, these assessments have drawn on literature data (such as energy efficiencies and technology costs) where reliable sources are available, which are supplemented by results of process simulation carried out in this work for less-studied subsystems (such as DRI and ammonia cracking).

2.1. System definition and cases for analysis

The prerequisites for green hydrogen-based steelmaking are abundant renewable energy, iron ore and water, which makes the Pilbara region of Western Australia a prime location. The fossil-free supply chain system following the H_2-DRI-EAF technical route was modelled to

produce 40 million tonnes of semi-finished steel (SFS) per year, based on current Australia-Japan iron ore trade, with both the iron ore and all the required energy sourced from the Pilbara region in Western Australia. The objective was to assess (and minimise) the system's energy consumption and green premiums – the difference in cost between one tonne of fossil-based steel and one tonne of hydrogen-based steel.

Twelve unique cases were studied with three key variables: supply chain (SC) design, energy vector and shipping fuel (liquid hydrogen (LH_2) or ammonia (NH_3)), and year (2030 or 2050), as detailed in Table 1. Alike Wood et al. [67], multiple energy and material trade alternatives were investigated, which consequently differed in the location of DRI, EAF and supporting production processes. SC1 followed the "traditional" route of Australia exporting energy and iron ore for iron and steel production in Japan, differing from present-day practice by substituting coal with hydrogen. SC2 exported the intermediary product between DRI (iron production) and EAF (steel production), called hot briquetted iron (HBI), along with hydrogen to complete steel production in Japan. Although DRI is an exportable commodity, it is prone to oxidation; in comparison, HBI removes the challenge of sealing the cargo in an inert gas atmosphere [26]. SC3 exported semi-finished steel to Japan, completing all iron and steel production processes in Australia. Under all cases, the premise is that either direct renewable energy, or hydrogen produced via renewable energy, must be utilised to energise the entire supply chain. Hence, hydrogen exports serve both energy and ore reductant requirements in Japan. The consideration of the two alternative energy vectors, LH_2 and NH_3, both among potential H_2 carriers for long-distance transport [66], was to allow a comparison between the two options within the context of a regional supply chain for decarbonised steel. In terms of the timelines, 2050 was selected to align with net-zero carbon targets under the Paris Agreement, with 2030 as a medium-term milestone for emission reductions.

The three supply chains are illustrated in Fig. 1, distinguished by processes during four discrete stages: Australian production, export preparation, marine transportation, and Japan production. For simplification, intermediary energy storage and conversion processes including compressed gaseous hydrogen (CGH_2) storage, fuel cell power generation and combustion for heat generation, are not shown. For all cases, the shipping route was from Port Hedland, Australia, to Port Osaka, Japan, quantified at 3497 nautical metres [50].

Across all the supply chain configurations, hydrogen (or NH_3 as an alternative form) has four critical end-use applications:

(1) **Feedstock**, to reduce iron ore to sponge iron in the shaft furnace.
(2) **Heat for production,** to provide thermal energy (converted via combustion) for production processes.
(3) **Power for production**, to provide electrical energy (converted via fuel cells) for production processes.
(4) **Transport,** to provide electrical energy (converted via fuel cells) to power electric motors which propel shipping vessels.

Besides this, hydrogen serves two critical energy storage roles: in the form of LH_2/NH_3 for long-distance transportation from Australia to Japan (as introduced above) and in the form of CGH_2 to provide a buffer between those processes to operate in Australia with a constant load and the variable renewable energy (VRE) supply (to be detailed in Section 2.2.1).

This work did not consider domestic transportation (and any associated intermediate storage) and loading/unloading at ports, which were deemed negligible compared to the major components of the system. Embodied emissions of related infrastructure have also been excluded.

Table 1
Variables applied within the twelve unique cases.

		Time period	2030		2050	
		Energy vector and shipping fuel	LH_2	NH_3	LH_2	NH_3
Supply chain design	SC1	Export **H_2** and **iron ore** for iron and steel production in Japan	SC1-LH_2-2030	SC1-NH_3-2030	SC1-LH_2-2050	SC1-NH_3-2050
	SC2	Export **H_2** and **HBI** for steel production in Japan	SC2-LH_2-2030	SC2-NH_3-2030	SC2-LH_2-2050	SC2-NH_3-2050
	SC3	Export decarbonised **steel** to Japan as semi-finished products (LH_2/NH_3 only required as shipping fuel)	SC3-LH_2-2030	SC3-NH_3-2030	SC3-LH_2-2050	SC3-NH_3-2050

2.2. Technical description and energy assessment

Here, the key characteristics of all the system components and the approaches adopted for energy assessment are presented. Further equations and parameters for energy modelling are detailed in Supplementary Information (SI), Section A.5.

2.2.1. Energy demand and renewable energy supply

Whilst constant diurnal renewable energy is ideal (e.g., sunny in the day, windy at night), the solar-dominant Pilbara region, like many other locations, delivers VRE. The 100% VRE systems were modelled in Homer Pro microgrid software which optimised for lowest net present value (NPV). Despite allowing for both solar and wind energy assets in the optimisation, all cases opted for a design with zero reliance on wind power. This meant that all the processes operating on the Australian side relied solely on solar irradiation available at the Pilbara site which has insignificant seasonal variation although the diurnal solar cycle is inevitable. The latter necessitated short-term (daily) energy storage to bridge (i) the constant power and/or H_2 demands of those inflexible processes operating in Pilbara and (ii) the VRE supply. Such processes included DRI (and the associated H_2 heating and compression), EAF and NH_3 synthesis. In contrast, flexible processes including electrolysis and H_2 liquefaction were considered to fully accomplish their daily load during the daylight hours and therefore did not require the aid of energy storage. Since a hydrogen buffer (to supply DRI and NH_3 synthesis) was an important part of the required storage capacity, CGH_2 (as opposed to other options such as batteries) was chosen for implementing the short-term energy storage. To provide a quantification of the diurnal distribution of energy demands by the flexible and inflexible processes, the 24-hour duration was divided into a daylight period (denoted by VRE_{on}) and a non-daylight period (denoted by VRE_{off}), with the length of the former set to 9 h which represents a conservative estimate as daylight hours in Pilbara are typically 10–12 h/day.

The daily demand for all flexible processes was met only during VRE_{on}, in unison with the dynamic VRE supply. An inflexible process, on the other hand, required constant energy and/or hydrogen feeds during both VRE_{on} and VRE_{off} with the latter period supplied by the CGH_2 storage. The total demand during the VRE_{on} period thus comprised both the demands of the flexible processes and that of operating CGH_2. Note that the consideration of flexibility concerns only the energy supply to the processes that occur on the Australian side of the supply chain; the processes to take place in Japan were always supplied by the energy shipped from Australia in either form of H_2 carrier (LH_2 or NH_3). To further illustrate the energy routing in the system, Fig. 2 shows three distinct energy pathways for one of the energy demands, H_2 as DRI reductant, depending on the process location and energy vector. Energy pathways for all end-use applications are detailed in SI, A.1.

It is worth emphasising that the two time periods (VRE_{on}, VRE_{off}) were defined solely for the purpose of composing the diurnal electricity demand profile for each case. The demand profile defined as such formed input to Homer Pro where the actual, location-specific (typical)

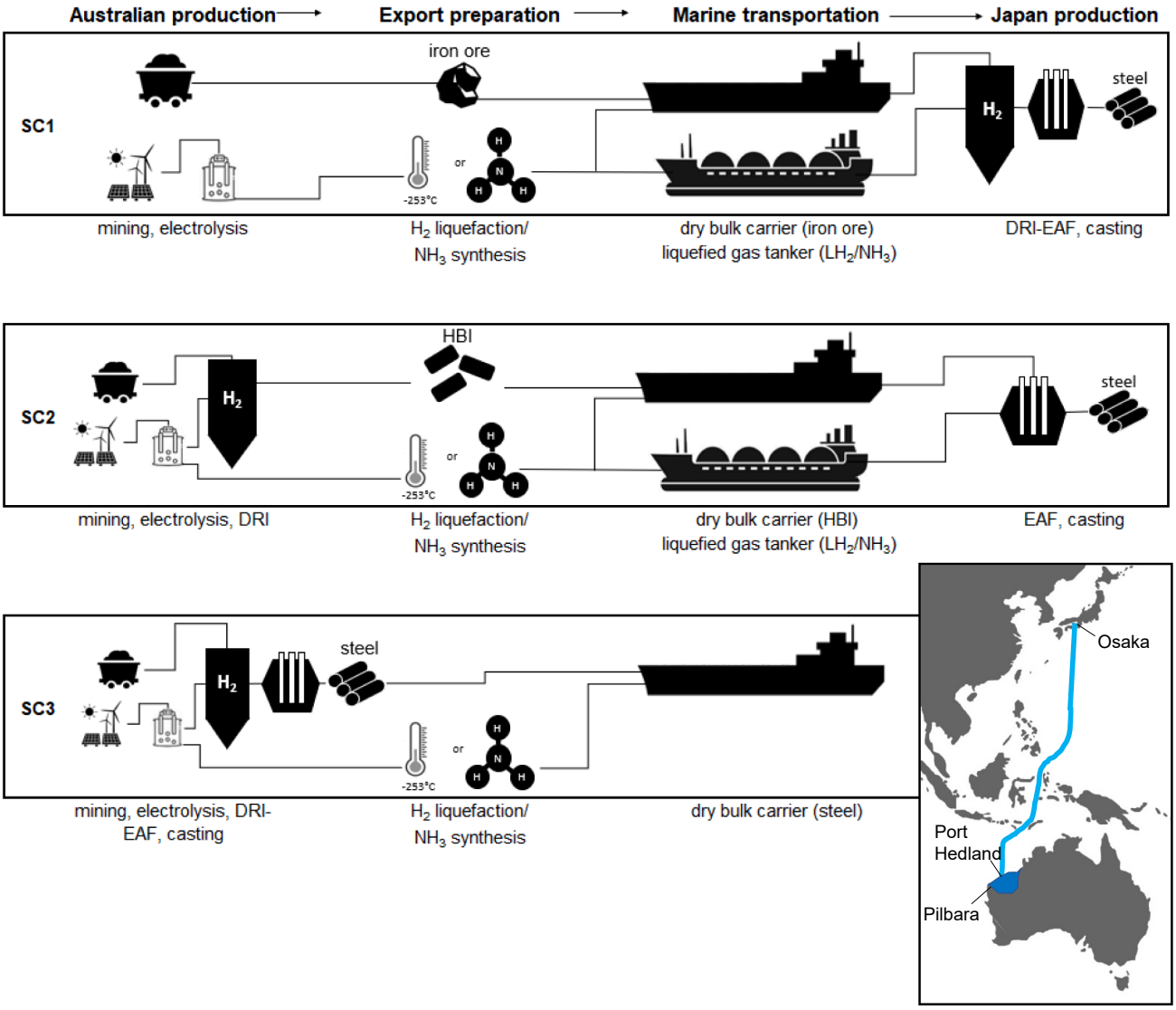

Fig. 1. Simplified supply chain illustrations, including map of shipping route (original map from [62]).

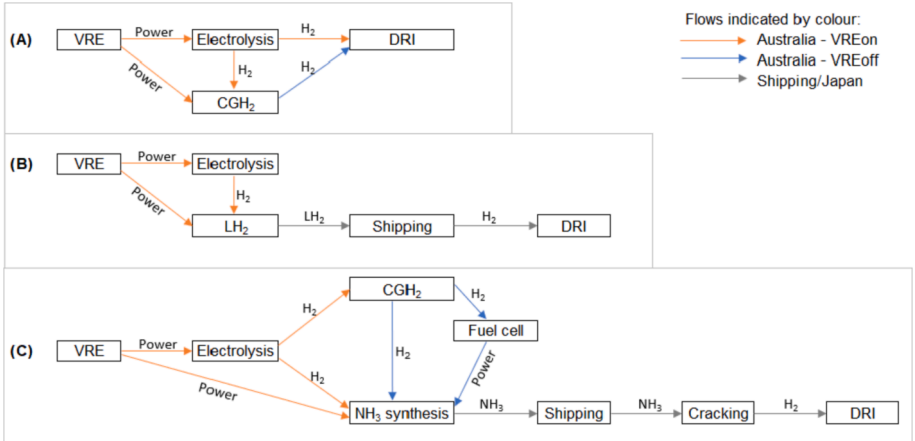

Fig. 2. Energy pathways for H_2 serving DRI as reductant, when DRI occurs in: (A) Australia, (B) Japan with LH_2 as the energy vector, and (C) Japan with NH_3 as the energy vector.

diurnal variation of the available renewable energy was used to compute the cost-optimal design of the renewable energy system that can satisfy the specified demand profile (see SI, A.2 for more details).

2.2.2. Iron and steel production

Iron ore, 95% hematite (Fe_2O_3) and 5% inert material by mass, is reduced by hydrogen in the shaft furnace, as shown in Equations (1)-(2), releasing only water [63].

$$Fe_2O3 + 3H_2 \rightarrow 2Fe + 3H_2O_{(g)} \quad (1)$$

$$Fe_2O3 + H_2 \rightarrow 2FeO + H_2O_{(g)} \quad (2)$$

The shaft furnace operates at 900 °C and atmospheric pressure, and the metallisation rate is taken as 94%. Before entering the furnace, H_2 is heated to 900 °C and compressed from 1 bar to 2 bar, to overcome the pressure drop in the shaft furnace. Using Aspen Plus Modelling (see SI, A.3), the energy consumption was calculated to be 0.45 MWh/t liquid steel (LS) for H_2 heating pre-DRI and 0.065 MWh/t LS for H_2 compression pre-DRI. The outputted sponge iron was either fed directly to the EAF or briquetted to produce HBI for export.

EAF power consumption was determined based on literature data, 2.4 MJ/kg LS [34], adjusted according to the chosen metallisation rate. Scrap, carbon, and lime additions were not considered in the EAF process. A continuous caster followed the EAF where blooms, billets and slabs were formed, the semi-finished state for further processing (not considered in this work). Casting energy demand was taken from literature data, 0.0103 MWh/t LS [31]. Overall, the following key material flow data were derived: 1.5 t ore/t steel, 1.1 t HBI/t steel and 52 kg H_2/t steel (note that hereafter, "steel" refers to "semi-finished steel"). Since these processes are either commercial or modelled with a theoretically rather optimal design in the case of DRI, none was considered to incur an efficiency improvement from 2030 to 2050.

Energy supply to these processes depended on their location and the timing. Thermal energy was either produced using electrical heating during VRE_{on} in Australia (with efficiency of 90%), or via H_2 (with H_2 from intermediate CGH_2 storage during VRE_{off} in Australia, or with LH_2 in Japan) or NH_3 (in Japan) combustion (with efficiency of 85% based on the lower heating value, LHV, of the fuel). Power was either directly served as VRE (during VRE_{on} in Australia) or indirectly through fuel cells fed with H_2 from intermediate CGH_2 storage (during VRE_{off} in Australia) or LH_2/NH_3 exports (in Japan). For energy carrier-to-power conversion, solid oxide fuel cell (SOFC) technology was used as an advantageous high-temperature operation suitable for stationary, large-scale power generation [39]. Additionally, SOFCs support the direct use of both hydrogen and ammonia, avoiding NH_3 cracking [38]. Stationary SOFC efficiency value of 60% (based on LHV) was used for 2030 [44,51] with modest increase to 64% in 2050.

2.2.3. H_2 production, storage, and conversion

Carbon-free hydrogen is produced via electrolysis of water using renewable energy. The alkaline electrolyser, chosen in the modelling, operates at a temperature of 70 °C and atmospheric pressure with efficiency of 68% in 2030 and 75% in 2050 [28]. The electrolyser design capacity of 86.5% is taken from industry data [58]. Based on a large-scale electrolyser size of 100 MW, 2.04 t H_2/hr and 2.25 t H_2/hr is achievable per module in 2030 and 2050, respectively.

Aboveground gaseous hydrogen storage in steel tanks at 150 bar (and 25 °C) was selected for short-term storage (CGH_2) due to its rapid ramp-up/down and high cycle lifetime [18], and uncertainty avoidance from alternative geological storage based on salt deposits or depleted gas reservoirs [19]. Steel is a common material for compressed gaseous hydrogen storage up to 250 bar [23]. Using Aspen Plus, compression energy demand was determined as 2.68 kWh/kg H_2 which aligns with literature [32].

Liquefaction of hydrogen gas requires intensive energy to reach temperatures less than −253 °C at a pressure of 1 bar. Commercial hydrogen liquefaction plants consume 30% of hydrogen's dispensable energy at 10 kWh/kg H_2 [6]. Future reductions for large-scale plants to 6 kWh/kg H_2 have been forecasted for larger plants with process improvements [1,6,55]. These two energy intensity levels were adopted for 2030 and 2050, respectively.

NH_3 synthesis energy demand, to drive the air separation and Haber-Bosch processes, was taken from literature as 0.7 kWh/kg NH_3 [43]. NH_3 cracking was required pre-DRI (SC1) as pure H_2 was necessary in the shaft furnace. The use of NH_3 as the direct reductant of iron ore [25] is possible, however rarely examined in literature and not applied in this model. Using Aspen Plus and a similar approach to Giddey et al. [20] (see SI, A.3), the cracking energy was modelled using an NH_3 conversion rate of 95%, H_2 recovery rate of 85% and heat recovery efficiency of 85%. Thermal energy consumption rate was determined to be 0.072 MWh/t NH_3, supplied by NH_3 combustion with overall cracker efficiency of 79%.

2.2.4. Shipping

Dry bulk carriers were used to transport iron ore, HBI and steel. Iron ore is a 'major bulk' commodity, generally shipped in capesize vessels (>100,000 dwt) as a minimum. Australia's iron ore producers are capped by berthing capacities at Port Hedland [46] and currently use Newcastlemax vessels [7]. The largest vessel that HBI is transported in is the panamax (65,000–99,999 dwt) [26], and the same has been assumed for steel as a comparable 'minor bulk' commodity [61].

A 160,000 m^3 liquefied gas tanker was used to transport LH_2 at −253°C and LNH_3 at −33°C within low-vacuum insulated spherical tanks [3]. Boil-off gas (BOG) was estimated at 0.2%/day for LH_2 [66] and 0.02%/day for NH_3 [3].

Shipping, a hard-to-electrify mobility sector, can utilise electrofuels with internal combustion engines (ICEs) or fuel cells (FCs) for propulsion power. Whilst development of large-scale electro-fuelled ICE systems may precede fuel cells with electric motors by 5–10 years (due to technology maturity of ignition engines) the higher-efficiency fuel cell technology will likely prove more economical in the long-term with the added benefit of no dangerous nitrogen oxide emissions [5]. Both LH_2 and NH_3 were investigated as marine shipping fuels and adopted the mobile FC with electric motor propulsion system.

The proton exchange membrane fuel cell (PEMFC) is the most mature H_2-powered fuel cell technology, advantaged by a low operating temperature, small module size and decreased costs. PEMFC operation is moderately efficient at 50–60%, however heat recovery is unfeasible and pure H_2 is required. This technology has been ranked first for marine applications across a broad range of criteria by the European Maritime Safety Agency [60]. For NH_3 fuel, the SOFC is more appropriate as pure H_2 inputs are not required, removing the need for NH_3 cracking. SOFC operates at high temperatures and can reach an efficiency of 85% with heat recovery, or 60% without [60]. Hence, H_2-PEMFC and NH_3-SOFC were chosen for modelling. In the absence of energy efficiency targets specifically for marine shipping applications of FCs, the U.S. Department of Energy targets for long-haul trucks were utilised; 68% in 2030 and 72% in 2050 [36].

To calculate specific fuel consumption (g/kWh) and return trip fuel consumption (t/journey), a similar method to that described by Kim et al. [33] has been adopted, both particular to the vessel's propulsion system at 85% load factor. The number of journeys required was distinct for each type of vessel (given a 90% carrying capacity) and export demand. BOG losses were considered for LH_2 and NH_3 as both fuels and energy exports (see SI, A.4).

2.2.5. Other energy demands

Iron ore mining and water desalination are additional external energy demands excluded from Homer Pro modelling as they are not considered unique to the decarbonised steel system assessed in this study. Ore mining and processing energy demand was taken from literature as 0.11 MJ/t ore [56].

Considering global water stress [52], especially in the Pilbara region [37], surface water supply is constrained and desalination is deemed a requirement for all cleaning, process, and cooling water (see SI, B.4) within the supply chain. Although desalination may not be necessary for process cooling water if antifouling treatments are applied [49] or electrolysis if technology becomes more adaptable [59], it was consistently applied across all water demands to produce a conservative estimate of energy consumption. Desalination energy demand of 5 kWh/kL was taken from the 140,000 m^3/day Perth Seawater Desalination Plant [64].

2.3. Economic assessment

A standard NPV method was used for calculating levelised cost of steel (LCOS) and levelised cost of hydrogen production, for each case over the 20-year project economic lifetime. The real discount rate was 7% given an annual inflation rate of 1.65% (2016–2020 average [48]) and all costs were equalised on an AUD (Australian Dollar) 2020 basis. Capital expenditure (CAPEX) included steel plant, electrolysers, CGH_2 plant (compressor and storage tank), LH_2 plant (liquefier and storage tank), NH_3 synthesis plant (air separation unit, Haber-Bosch process, and storage tank), NH_3 cracker and stationary fuel cell stacks. Operational expenditure (OPEX) included electricity, ship charter (which excludes fuel as it is always derived from electricity), iron ore, labour, water, and infrastructure maintenance (2% of CAPEX). The costing approach treated electricity and shipping charter as externally procured resources since in principle, they need not be explicitly built for decarbonised steel and are more simply expressed in a $/unit basis. Homer Pro modelling determined the levelised cost of electricity (LCOE) as well as the energy system infrastructure CAPEX. Charter rates were determined based on the vessel, propulsion system and fuel storage CAPEX plus the OPEX of crew, port fees, consumables, maintenance, repair, and insurance. LH_2 or NH_3 shipping fuel production was incorporated within the overall energy system demands. For detailed economic modelling data and equations refer to SI, Sections A.6-A.10.

Fuel cells costs are expected to improve simultaneously with efficiency and lifetime. Stationary SOFC cost data was given by Whiston et al. [65] who evaluated U.S. DOE targets, with lifetimes up to 90,000 h [27] assumed for 2030 and an increase to 100,000 h for 2050. For long-haul mobile FC applications, the U.S. Department of Energy targets of 25,000–30,000 h lifetime and US$80–60/kW from 2030 to 2050 [36] were utilised, however these are in reference to mobile H_2-PEMFC stacks. For mobile NH_3-SOFCs, a hybrid approach has been taken for data selection to make the best use of available data; equal lifetime (and efficiency) as mobile PEMFCs, with equal costs as stationary SOFCs which is more representative of the technology's financial burden. Any improvement in lifetime positively affected the overall cost by reducing frequency of replacement within the 20-year project lifetime.

3. Results and discussion

In this section, the energy consumption, and financial costs per tonne of green steel are first presented, then those for establishing and operating the entire system. This is followed by more detailed insights from energy and cost perspectives before further issues are discussed.

3.1. Energy intensity and levelised cost of green steel

The two key outputs from the assessment – energy and cost demand of fossil-free steel – are firstly summarised overall and then compared to fossil-based steel.

3.1.1. Results overview

This study predicts that, depending on the case settings, one tonne of steel in 2030 will demand 5.4–8.6 MWh of electricity and cost A$913–1284, reducing in 2050 to 4.9–7.6 MWh and A$716–948. Across all the studied cases, significant improvement in the resource intensity and the levelised cost of fossil-free steel was projected with increasing supply chain concentration in Australia, as shown in Fig. 3. Thanks to the co-location of energy and steel production, SC3-LH_2 and SC3-NH_3 were the optimal cases which are closely aligned due to the minor influence of shipping fuels and energy vectors. On average, steel produced

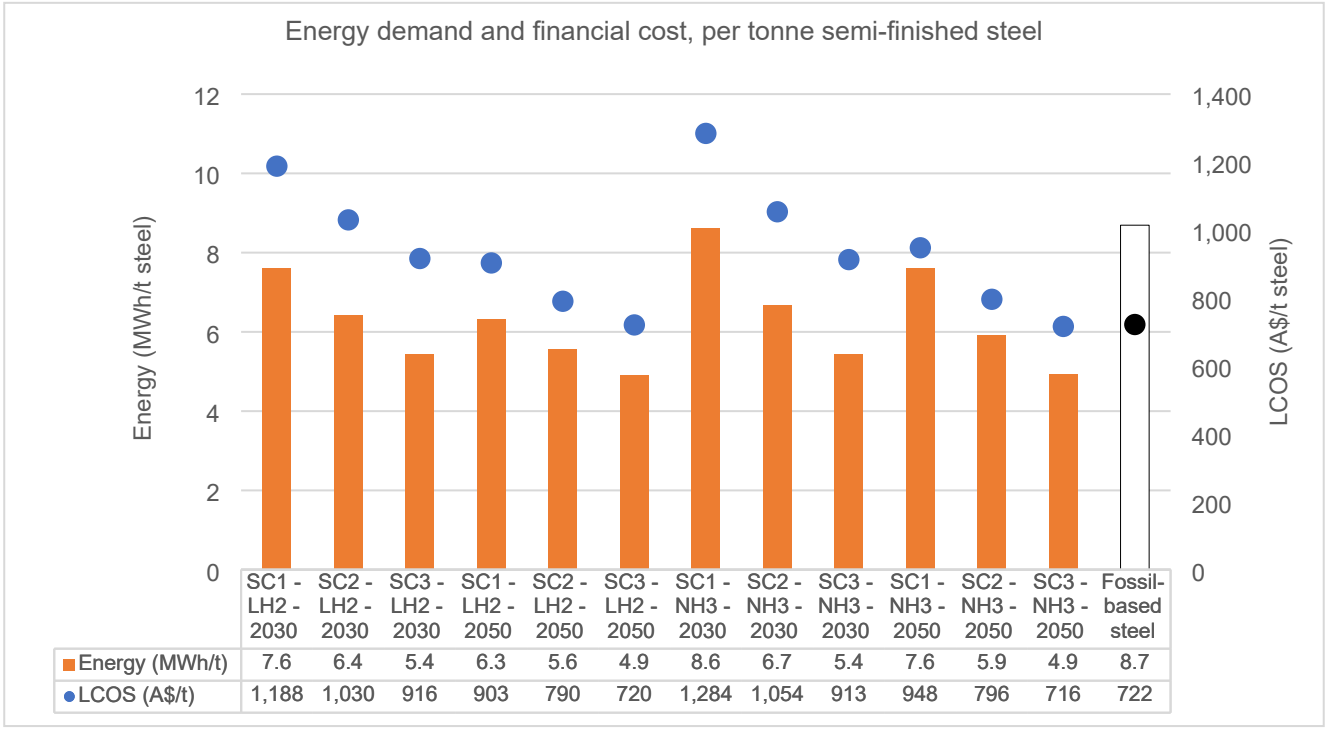

Fig. 3. Energy demand and financial cost per tonne of semi-finished steel.

via SC1 (iron ore and energy exports) and SC2 (HBI and energy exports) were 45% and 19%, respectively, more energy intensive than SC3. Clearly, the additional energy-consuming processes for LH_2 and NH_3 production in these supply chains with greater transport requirements and energy conversion losses burdened the resource systems. By using LH_2 instead of NH_3 for SC1, energy consumption was reduced by 12% in 2030 and 17% in 2050 with costs reduced to about 8% in 2030 and 5% in 2050. Compared to 2030 and depending on the supply chain and energy vector, process efficiency improvements realised in 2050 reduced energy consumption by 9–17%, while the combined effect of lower energy consumption (due to the improved efficiencies) and technology cost reduction led to the reduction of the levelised costs by a more substantial 21–26%. In particular, LH_2 energy consumption dropped markedly due to the projected improvement of liquefaction efficiency.

The results demonstrate that co-location of mineral and energy inputs with manufacturing processes positively benefits the system in terms of energy- and cost-efficiency. This suggests that strategic supply chain design is advantageous to investors and customers alike to decrease costs and accelerate market competitiveness.

3.1.2. Comparison to fossil-based steel

Commercial fossil-based primary steel is resource intensive. Considering raw material acquisition, iron and steel manufacturing, and related transport (lifecycle assessment modules A1-A3), one tonne of average Australian hot-rolled steel using the BF-BOF route emits about 3 t CO_2 and consumes 9 MWh of energy [8,35]. According to the best case predicted in this study, (green) hydrogen-based steel supply chains can remove the carbon emissions arising from fossil fuel powered operations whilst limiting energy consumption to 5 MWh (the energy for hot rolling which proceeds casting is additional, although a relatively minor contributor). These results rely on spatial proximity between renewable energy resources, iron ore deposits and the H_2-DRI-EAF plant, as well as the realisation of projected technology development from 2030 to 2050.

Today's price of steel is highly volatile, yet it can be approximated at A$722/t for semi-finished products [54]. Hydrogen-based steel can reach price parity by 2050 for the two optimal cases with Australian-based iron and steel production (SC3). Exporting energy and HBI (SC2), or energy and iron ore (SC1), from Australia reduces the likelihood of market competitiveness. In 2030, a regional carbon price between A$66 and A$192/t CO_2 will be necessary to make green steel competitive (based on the average 3 t CO_2/t steel emitted from Australian produced primary steel). In 2050, the prospective carbon tax threshold is reduced significantly to about A$70/t CO_2 for SC1 and A$25/t CO_2 for SC2, diminishing to zero for SC3.

3.2. Overall energy and financial burden of establishing and operating the decarbonised steel supply chain

The scale of the decarbonised solution for an annual throughput of 40 Mt is considerable. The system energy requirements are 195–343 TWh per year, ranging from the most (SC1-NH_3-2030) to the least (SC3-LH_2-2050) demanding cases. This constitutes 74–129% of Australia's total electricity production [14]. In terms of physical capacity, 126–230 GW solar PV panels, 48–96 GW of electrolysers, and 2–3 desalination plants (operating at 140 ML/day) will need to be installed.

GW-scale energy interventions demand billion-dollar investments. As shown in Fig. 4, in 2030, the magnitude of capital for SC3 (mean A$202 billion) is advantageous compared to SC2 (mean 23% increase) and SC1 (mean 56% increase). By 2050, SC3 capital demands shrink due to reducing technology costs by 32% to A$137 billion, facilitating widespread investments and access to commercial markets. On average, 50% of initial capital is required for the solar power plant, 48% for the H_2-iron-steel plant and a minor 2% for the shipping vessels (which excludes fuel cell replacement costs due to negligible influence, as well as water desalination and ore mining CAPEX).

In the comparison of energy vectors, LH_2 cases need less capital than NH_3 equivalents, mainly due to reduced solar power capacity, a relationship most prominent in SC1 with 16% solar CAPEX reduction in 2030 and 21% reduction in 2050; benefits of LH_2 systems increase with

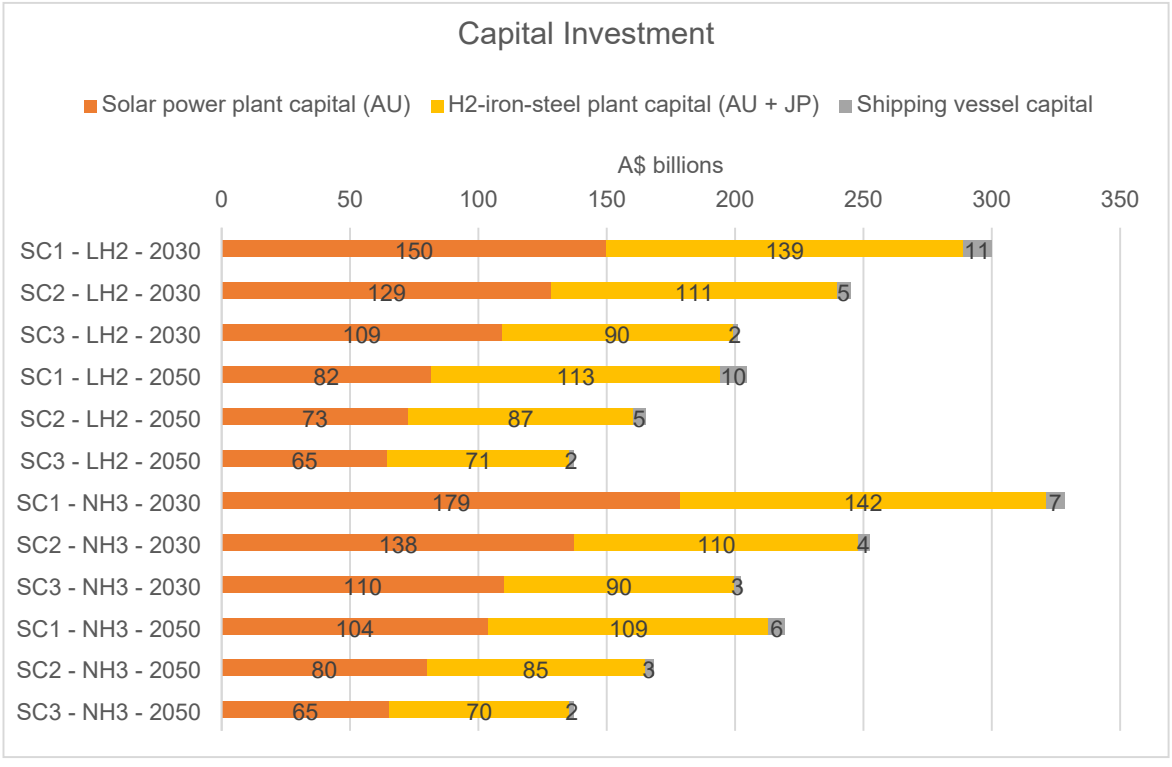

Fig. 4. Capital required for energy and production systems.

time as liquefaction efficiency improvements are realised. Similarly, SC2 solar CAPEX reduces by 7% in 2030 and 9% in 2050 in favour of LH_2, although SC3 differences are negligible. In contrast, fewer liquefied gas tankers are needed for NH_3 due to improved volumetric energy density, reducing the shipping vessel CAPEX.

The above results show the significant energy and financial stress caused by a production system of this scale. To mitigate this stress, supply chains with co-located iron and steel manufacturing, renewable energy and iron resources should be the foremost priority, coupled with the choice of energy carrier based on quantitative evidence. Despite the investment cost reductions acclaimed in 2050 compared to 2030, the decarbonised system requires investment in the next decade to avoid carbon lock-in. This would mean a large financial barrier to be tackled, a challenge further compounded by the consideration of investment losses on existing fossil-based assets.

3.3. In-depth examination of energy consumption

Sankey Diagrams were developed to illustrate energy distribution flows; renewable electrons travelling from VRE (start node) to processes based in Australia (light blue nodes) and Japan (dark blue nodes). 2030 cases (Fig. 5) follow very similar relationships to 2050 cases (SI, B.1), although with benefits of process efficiency improvements for electrolysis, liquefaction, and fuel cells. In each diagram, one can see, from left to right, how the VRE was consumed directly by processes that operate in Australia during VRE_{on} and how subsequently the energy flows were re-distributed towards (1) those processes operating in Australia during VRE_{off} (in all SCs except SC1-LH_2), (2) shipping (in all SCs) and (3) the processes operating in Japan (in SC1 and SC2). In all the cases, the centrality of electrolysis is evident in energy consumption, as expected, although diminishing in significance with time (2030 to 2050) and supply chain (SC1 to SC2 to SC3). With LH_2, new energy cost was incurred by the introduction of CGH_2 when moving from SC1 to SC2 due to the operation of the (inflexible) DRI process in Australia, but the overall energy cost for energy vector production and for transport was significantly reduced; this trend contributed when moving from SC2 to SC3. On the other hand, the inflexibility of ammonia synthesis, in the NH_3-based cases, increases the energy storage (CGH_2) requirement in coping with VRE. Furthermore, Japan-based processes (i.e., dark blue nodes which include energy to carry out processes, and the shipping fuel to transport energy to, Japan) drive up energy demand, especially prevalent for DRI in SC1-NH_3 where NH_3 cracking is also required. These extra energy costs made LH_2 a more efficient energy vector overall, even though NH_3 as an energy carrier required fewer vessel-trips for transporting energy from Australia to Japan (thanks to its 1.7-times greater volumetric energy density) and suffered lower BOG losses than LH_2 (refer to SI, B.2).

Fig. 6 further compares the intermediate- and end-users across the 12 cases. The end-use categories cover production feedstock (reductant for DRI), major production energy (EAF, H_2 heating pre-DRI), minor production energy (H_2 compression pre-DRI, casting, iron ore mining and water desalination) and shipping fuel (transport). Intermediate processes cover CGH_2 storage in Australia, and H_2 liquefaction/NH_3 synthesis for exports and shipping fuel. For each category, energy

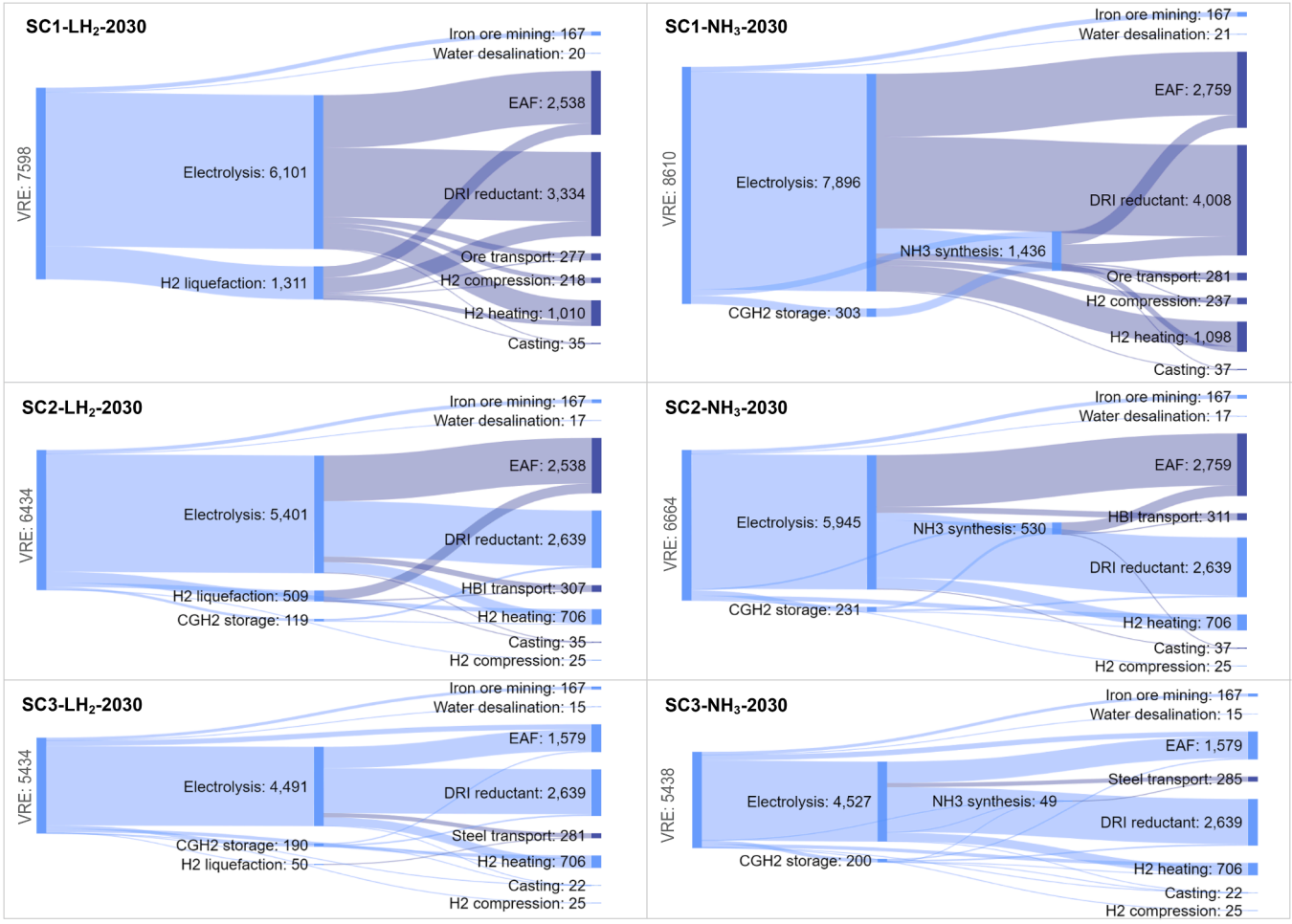

Fig. 5. Sankey energy distribution diagrams for 2030 cases (refer to SI, B.1 for 2050 cases) *Note: data in kWh/t steel; may not sum due to rounding to nearest whole number; node width correlates to magnitude of energy demand; scale is normalised for all cases.*

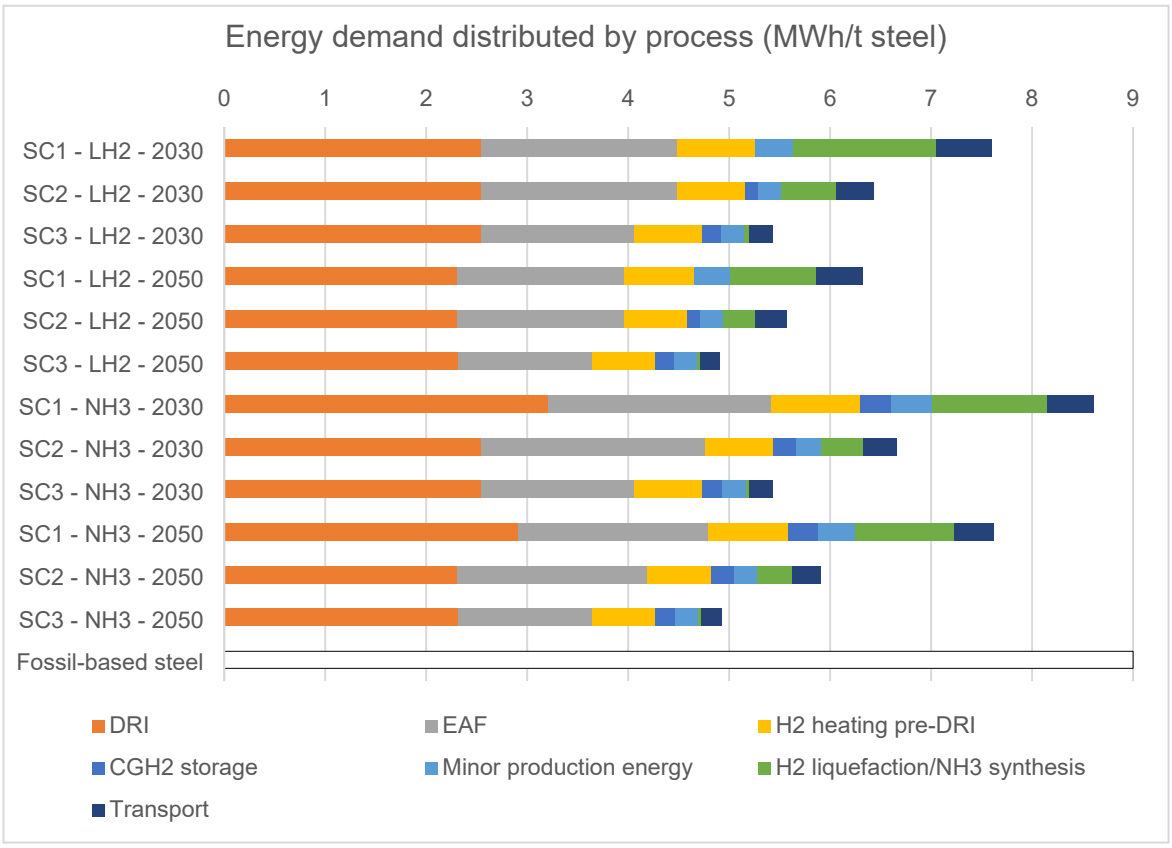

Fig. 6. Energy distribution per tonne of semi-finished steel.

consumption represents either direct consumption of VRE (for processes running in Australia during VER_{on}), the VRE consumed for producing the portion of H_2 that eventually gets consumed in the category (processes running in JP and transport), or a combination of both (processes running in Australia during both VRE_{on} and VRE_{off}). As shown in Fig. 6, the most energy-intensive end-use processes are DRI (using H_2 as the reductant) and EAF, representing on average 41% and 28%, respectively, of total demand. If DRI reductant and pre-DRI processes (H_2 compression and H_2 heating pre-DRI) were incorporated, the complete DRI process contribution would increase to 53% (not shown in the chart). From 2030 to 2050, gains in electrolyser, liquefaction and fuel cell efficiency reduce energy demand appreciably.

Further, Fig. 6 shows that H_2 liquefaction/NH_3 synthesis constitutes an average 15% of total energy demand for SC1 where energy exports are deeply depended on, diluting to 7% for SC2 and 1% for SC3. H_2 liquefaction, as an isolated process, is initially more energy intensive than NH_3 synthesis as efficiency improvements have not yet been realised; SC1-LH_2 sees relative reduction in energy demand from 19% of total in 2030 to 13% in 2050 (whilst NH_3 stays at 13%). However, SC1-NH_3 requires cracking pre-DRI; summing such energy demand (absorbed in the DRI portion in Fig. 6) to the burden for synthesising the energy vector increases accountability for these cases (2030 and 2050) to 21%. Transport (i.e., shipping fuel) is a minor overall contributor (average 5%) with any changes mainly due to the transportation of energy (LH_2 or NH_3) as opposed to material. This is due to negligible differences in material export demands between supply chains; iron ore, HBI and steel all require approximately 5 kg H_2/t steel (in the form of LH_2 or NH_3) for dry bulk carrier fuel.

Pathway process efficiency, from VRE to end-use application, can demonstrate the degree to which LH_2 is advantageous over NH_3 (as shown in Table 2 for the major end uses). Inflexible NH_3 synthesis calls for intermediate CGH_2 storage and fuel cells to provide power in non-daylight hours (62% of the day) and using NH_3 as a H_2 carrier demands cracking pre-DRI, driving up process inefficiency. The efficiency gap increases in 2050 due to the substantial reduction in energy demand projected for H_2 liquefaction (down 40%).

Table 2
Pathway efficiencies for most energy-demanding end-users (MJ VRE required/MJ delivered to end-user).

	In Australia		In Japan - LH_2 exports		In Japan - NH_3 exports	
	2030	2050	2030	2050	2030	2050
DRI (H_2 reductant)	66%	72%	52%	61%	43%	48%
EAF	48%	54%	30%	37%	27%	32%
H_2 heating pre-DRI	63%	68%	44%	52%	41%	45%

In summary, the detailed analysis of energy consumption shows the relative importance of different components in the supply chain and how their locations affect their energy demands, with the latter shaped in part by the comparative performance of the two energy vectors which itself is also affected by the supply chain configurations. Overall, these results show that energy losses are gross for both energy vectors in the processes located in Japan, and that co-location of renewable electrons and H_2-iron-steel manufacturing plant delivers immediate energy efficiency benefits.

3.4. In-depth examination of economics

Costs are investigated through a detailed lens for the levelised cost of steel, complemented by the levelised cost of electricity and hydrogen as the core constituents of the fossil-free production system.

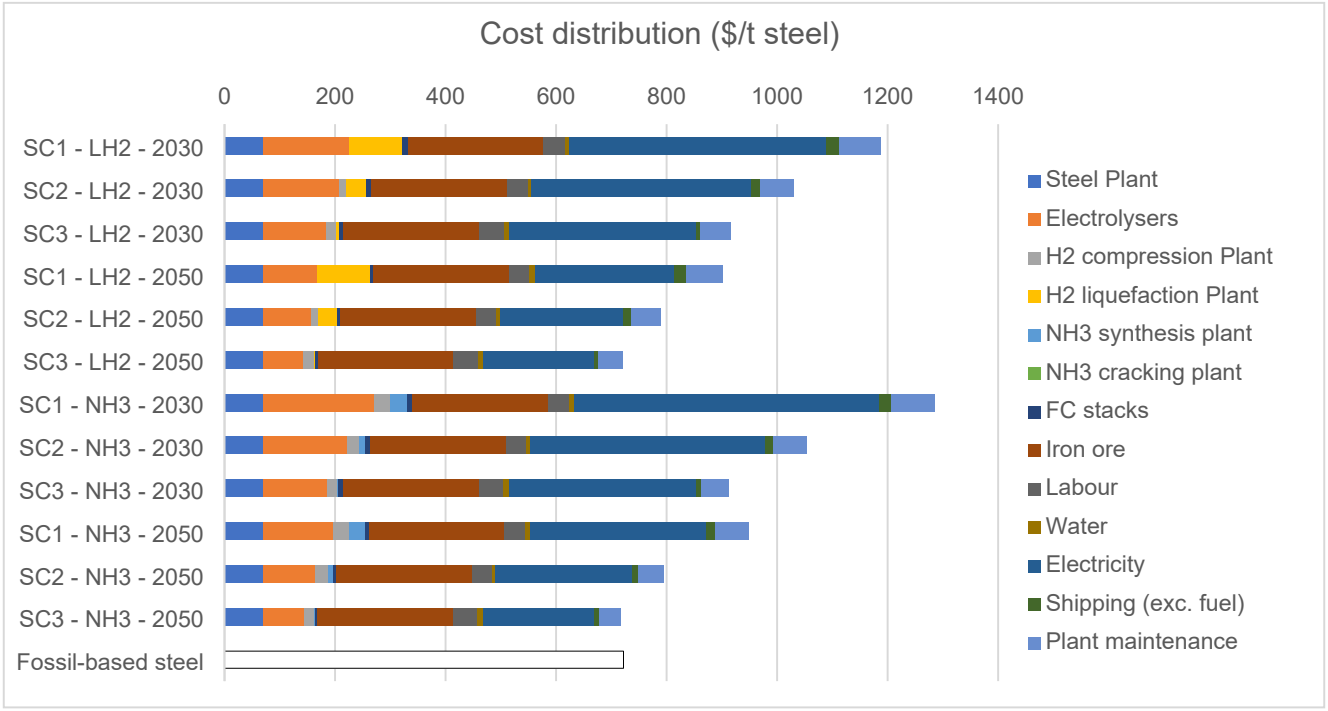

Fig. 7. Cost distribution per tonne of semi-finished steel.

3.4.1. Levelised cost of steel

The LCOS for each case is shown in Fig. 7, separated by key expenditures comprising ~ 25% CAPEX (infrastructure) and ~ 75% OPEX (iron ore, labour, water, electricity, shipping, and plant maintenance). The energy-intense nature of the hydrogen-based steel production supply chains is reflected in the costs; electricity accounts for 28–43% of the total. This exceeds current fossil-based production where 20–25% of total costs are required for energy [24], indicating a shift in revenue dynamics; cheap renewable electrons are central to profitable fossil-free steel. Absolute electricity costs ranged from A$200/t (SC3-2050) to A$550/t (SC1-NH_3-2030), depending on the electricity demand and LCOE.

For CAPEX, electrolysers were the dominant cost factor, accounting for 12% of costs on average, a function of hydrogen demand, electrolyser efficiency and electrolyser unit cost. Influentially, electrolyser efficiency improved by 10% and unit cost reduced by 35% from 2030 to 2050. Regarding hydrogen demand, SC3 consistently required 0.09 t H_2/t steel which increased to an average of 0.11 t and 0.014 t for SC2 and SC1, respectively. Additionally, NH_3 was 29% more hydrogen-intense than LH_2, decreasing to 10% and 1% for SC2 and SC3, respectively.

In terms of H_2 conversion and storage, NH_3 supply chains were more energy-intense however less capital-intense than LH_2 equivalents (encompassing CGH_2, LH_2 and/or NH_3 plant). For SC1, the average LH_2 case dedicated 9% of costs to H_2 conversion and storage infrastructure, compared to 5% for the NH_3 case. CAPEX differences reduced with dilution of export demands, equalising at 3% of total costs for both energy vectors in SC3.

Regarding OPEX, iron ore maintained a constant value of A$246/t across all cases, accounting for a 19–34% of the total. Note that market ore prices are highly volatile however will uniformly affect all cases. Plant maintenance, labour, shipping, water, and fuel cell stacks accounted for, on average, 6%, 3%, 2%, 1% and 1% of total cost.

The results correlated reasonably with literature; Wood et al. [67] estimated hydrogen-based steel, shipped as a semi-finished product from Australia to Japan (i.e., SC1) in an arbitrary future year, to be A$937/t, close to this study's average SC1-2030 cost of A$914/t (differences may be attributed to Wood's assumption of A$2/kg H_2 and use of fossil-fuelled shipping). Gielen et al. [21] determined, using a top-down method, one tonne of hydrogen-based to be around A$100/t more expensive than fossil-based steel when HBI was exported from Australia (i.e., SC2), not far off this study's results of approximately A$70/t for SC2-2050, calculated using a bottom-up method.

3.4.2. Levelised cost of electricity

The LCOE computed using Homer Pro and CSIRO projection data for solar CAPEX [22] was on average A$59/MWh for 2030, which decreased appreciably to A$39/MWh for 2050 with solar PV panel cost reduction (down 66%) (see SI, B.3). In comparison, the LCOE computed by Graham et al. [22] for utility-scale solar PV with similar CAPEX projection data was A$30–55/MWh in 2030 and A$25–45/MWh in 2050. The difference between these LCOE estimates is mainly due to the capacity factor of solar PV installation. In this work, the underlying capacity factor values were calculated by Homer Pro energy modelling specifically for the case study location, which was 21% on average (based on 22 years of historical solar irradiation data in the Pilbara), whereas the low-range LCOE values from Graham et al. [22] were determined using a higher capacity factor of 32%. Nevertheless, the sensitivity of the LCOE to this study's results was limited; if the LCOE did decrease by 10%, the LCOS would decrease by approximately 3%.

The relationship between electricity demand, process flexibility and variable solar supply altered the LCOE between supply chains and energy vectors marginally; the higher the storage capacity during daylight hours (see SI, A.2) as a percentage of daily load, the greater the flexibility available to the VRE system and hence lower the LCOE. The optimised case was SC1-LH_2-2050 at A$37/MWh, reflecting the most flexible system with competitive solar panel costs. LCOE was slightly improved for LH_2 cases, reduced in comparison to the NH_3 equivalent by 5% and 3% for SC1 and SC2, respectively, then diminishing to 0% for SC3.

3.4.3. Levelised cost of hydrogen production

The optimal hydrogen production costs exceeded the Australian government's 'H_2 under $2' goal [16], despite 40% reduction over two decades; A$2.94/kg H_2 in 2050 and A$4.75/kg H_2 in 2030. The slight

variations between supply chains and energy vectors echoed trends in LCOE. Costs were dominated by electricity (65%) and electrolyser CAPEX and maintenance (33%), the remaining due to water and labour. 2050 cases evidently benefited from the reduction of electrolyser CAPEX (down 28%) and LCOE (down 35%) yet costs on a 'per unit' basis were still rather high due to the limited electrolyser utilisation rate of 37.5%. The relationship between daily hydrogen demand and rated electrolyser capacity is critical: an improved electrolyser utilisation rate drives down costs; however, it is only achievable in a region with optimal, more evenly distributed diurnal renewable energy.

3.5. Further discussion

The above results and discussion have focused on energy, however, the sheer scale of the green steel production assessed in this work means other resources, particularly water and land, could also be impacted. A preliminary understanding was thus developed (see SI, B.4) of the system's water and land consumption. The processes demanding the greatest amount of water were electrolysis, consuming 9L/kg H_2, as well as the EAF and continuous caster, consuming 1.6kL and 1kL/t steel, respectively [31,69]. Net consumption was offset by return water received during DRI and FC power production, if co-located with water electrolysis. This resulted in an annual water demand of 115-169GL across Australian and Japanese operations (depending on the case), equivalent to 80–118% of the Pilbara region's water consumption (based on the most recent available data [37]). Following a similar method, the system's land footprint was calculated with the dominating footprint from solar panels, quantified at 28,000 m^2/GW, largely determining the results. Based on Australian operations (due to the unifying system condition of energy production in Australia), the system's land consumption was determined to be 3500–6400 km^2 (depending on the case), equivalent to 0.7–1.3% of the Pilbara region's land area. Whist this footprint is not technically an issue considering Australia's large land mass, it would require consideration in Japan as its entire area as a country is 25% lower than the Pilbara region [40,45]. The range of results for both water and land consumption followed the same trends as energy consumption; co-location of production processes and renewable energy resources reduced system burden, as did the use of LH_2 over NH_3, and 20 years of technology development to 2050. It should be noted that land costs were not considered in the economic model however are likely to follow the trends of land consumption. Moreover, securing renewable energy sites in optimal locations with sufficient land area and water resources are crucial first steps in operation establishment. Limiting production system stress placed on finite water and land resources is supported by localised, energy-efficient supply chains.

There is inevitable uncertainty in dealing with future scenarios and simplifying model assumptions. The accuracy of the energy and economic model is contingent on the accuracy of original data projections. To reduce errors, recent data from reputable organisations and authors were sought and compared, whilst various processes were modelled from first principles using Aspen Plus. Furthermore, the inclusion of two timelines (2030 and 2050) effectively allowed the assessment of the impact of several technical and economic parameters that were projected to improve over time. To gain a deeper understanding of the impact of various independent variables on the dependent variables including energy consumption and LCOS, a sensitivity analysis was conducted of key process efficiencies for 2050 cases, all varied ± 5% from the base case (see SI, B.5). Electrolysis efficiency was found to be the most influential on both energy demand (±4% on average) and LCOS (±2% on average) across all supply chains, followed by fuel cell efficiency (average ± 2% energy and ± 1% LCOS). Due to energy vector significance, SC1 was most sensitive to liquefaction efficiency (±3% energy and ± 2% LCOS), reducing in impact for SC2 (±1% energy and ± 0.5% LCOS) to almost nil for SC3. Similarly, SC1 was most sensitive to NH_3 synthesis efficiency though to a lesser extent (±1% energy and ± 0.5% LCOS), reducing to approximately zero for SC2 and SC3. Reflecting on these uncertainty ranges, the differences between NH_3 and LH_2 for SC3 are considered negligible for SC3 (±0% energy, 1% LCOS), however still visible for SC1 (±14% energy, ±6% LCOS) and SC2 (±5% energy, ±1% LCOS). If LH_2/NH_3 process efficiency variation exceeded ± 5% from the assumed data points, resultant energy vector relationships may change. For each of the 12 cases the LCOE varied only marginally during the sensitivity analysis, due to the largely unchanged ratio of storage capacity to daily load (representing VRE system flexibility).

Several other assumptions adopted by this study warrant further discussion. Firstly, the range of DRI products – hot-DRI, cold-DRI and HBI - should be considered in detail, including the distinct energy burdens and transportation challenges. This study omitted the additional energy burden of HBI pre-heating in the EAF based on the assumption that this requirement could at least in part be met by the recycled heat from the EAF. Nevertheless, this omission could lead to slight underestimation of (but without affecting the qualitative conclusion on) the advantages acclaimed from co-locating DRI and EAF facilities. Secondly, "Instant" establishment of the decarbonised supply chains was assumed at each of the two timelines. A transition period will be needed instead of a sudden switch, which can have important implications in terms of investments and the deployment of technical facilities and have not been considered in this work. It should also be noted that system efficiency could be improved by improving the operational flexibility of those processes considered here as inflexible, through better synchronisation between VRE supply and manufacturing as shown in other renewables-driven processes [9]). Finally, BOGs were accounted for as mass losses. However, they could be contained using an integrated re-liquefaction system, where energy is required to re-liquefy the gas and send it back to the tank as a cool liquid [2]; energy losses estimated for such a system may deviate from the mass losses considered here, although the impact to the overall energy efficiency is unlikely to be significant.

4. Conclusions

Harmful CO_2 emissions can be decoupled from the complete iron and steel supply chain through production and transportation systems based on renewable energy and green hydrogen. The system's resource and financial burden will vary appreciably with supply chain design, energy vector, and time; managing these variables is crucial for accelerating steel sector decarbonisation and market competitiveness with fossil-based alternatives. Under an Australia-Japan strategic partnership, this study assessed 12 future scenarios which led to the following key conclusions regarding the decarbonised steel energy system:

(1) Locating fossil-free steel manufacturing close to high-quality renewable energy and iron ore resources is advantageous from both an energy-efficiency and affordability perspective. If Australia's reputation as an energy exporter is not disrupted (i.e., SC1 with Japan-based production), energy demand per tonne steel will be on average 45% more onerous than that of a more climate-positive manufacturing economy (i.e., SC3 with Australia-based production), with costs 32% higher. Optimising geographical assets, in a collaborative regional approach, will accelerate the transition to net zero.

(2) Price parity is achievable by 2050 with minimal energy exports, but not likely in 2030 (mean period cost difference is 23%). Although the 20-year period will benefit from increased electrolysis, H_2 liquefaction and fuel cell power efficiencies, as well as emerging technology cost reductions, deploying market price signals before 2030 is critical to avoid carbon lock-in from long-term industrial assets. The necessary carbon price to mitigate green premiums is in the range of A$66–192/t CO_2 in 2030, and A$0–70/t CO_2 in 2050.

(3) LH_2, compared to NH_3, may prove a more energy efficient and cheaper energy vector, particularly in the long-term when liquefaction efficiency improvements are realised. If iron ore and H_2 are exported to Japan from Australia (i.e., SC1), an LH_2-based, compared to NH_3-based, production system in 2050 may beneficially reduce the energy demand

by 17%, and costs by 5%. These relationships mainly reflect the inflexibility of the Haber-Bosch process for NH_3 synthesis paired with variable renewable energy, as well as the additional energy burden of NH_3 cracking pre-DRI.

(4) Establishing a zero-emission production system will only be enabled by copious natural and financial capital, which must be secured early and managed judiciously. Within the (Pilbara) Australia-Japan setting, producing 40 Mt of decarbonised steel annually requires A $137–328 billion in capital investment for solar power, production, and shipping vessel infrastructure, and an annual 195–343 TWh of electricity. Given the system proportions, incremental scaling-up of the system would be a necessary path to the net-zero carbon goal.

This study on energy- and cost-effective clean energy provision for steel supply chains has produced informative results with implications for global industrial and public sector investments, especially in energy planning and carbon policymaking. Lessons learnt from the Australia-Japan case study can be related to regional alliances around the world, where the geographical integration of energy and iron ore resources should drive green steel markets.

A plethora of studies may proceed this work. Whilst energy and economics were the foci for this study, broader political, environmental, and social criteria need assessment, especially employment shocks from supply chain disruption and embodied carbon of the system's infrastructure. It must be acknowledged that political factors of industrial dislocation between nations is not addressed in this study. In this regard, SC2 with shared value-adding manufacturing between involved regions may be an appropriate medium to manage potential conflicts. Still requiring attention is work on the transition to peak production of green steel at large scale, exploring how to enable supply chains and facilitate just transitions through industrial strategies, policy, and regulatory frameworks.

CRediT authorship contribution statement

Alexandra Devlin: Conceptualization, Methodology, Analysis, Writing – original draft. **Aidong Yang:** Conceptualization, Supervision, Validation, Writing – review & editing.

Declaration of Competing Interest

The authors declare that they have no known competing financial interests or personal relationships that could have appeared to influence the work reported in this paper.

Acknowledgements

Financial support for AD during her PhD studies by the General Sir John Monash Foundation, and advice provided by Barbara Rossi, Rene Bañares-Alcántara and Robert Lean, are greatly appreciated.

Data availability

All energy and economic input data are referenced within the main text or Supplementary Information. Renewable energy supply data was obtained using Homer Pro microgrid software.

Appendix A. Supplementary data

Supplementary data to this article can be found online at https://doi.org/10.1016/j.enconman.2022.115268.

References

[1] Aasadnia M, Mehrpooya M. Large-scale liquid hydrogen production methods and approaches: a review. Appl Energy 2018;212:57–83. https://doi.org/10.1016/j.apenergy.2017.12.033.

[2] Ahn J, You H, Ryu J, Chang D. Strategy for selecting an optimal propulsion system of a liquefied hydrogen tanker. Int J Hydrogen Energy 2017;42(8):5366–80. https://doi.org/10.1016/j.ijhydene.2017.01.037.

[3] Al-Breiki M, Bicer Y. Technical assessment of liquefied natural gas, ammonia and methanol for overseas energy transport based on energy and exergy analyses. Int J Hydrogen Energy 2020;45(60):34927–37. https://doi.org/10.1016/j.ijhydene.2020.04.181.

[4] Andersson J, Krüger A, Grönkvist S. Methanol as a carrier of hydrogen and carbon in fossil-free production of direct reduced iron. Energy Convers Manage 2020;X:7. https://doi.org/10.1016/j.ecmx.2020.100051.

[5] Ash N, Scarbrough T. *Sailing on solar - could green ammonia decarbonise international shipping?*; 2019.

[6] Berstad D, Skaugen G, Wilhelmsen Ø. Dissecting the exergy balance of a hydrogen liquefier: analysis of a scaled-up claude hydrogen liquefier with mixed refrigerant pre-cooling. Int J Hydrogen Energy 2021;46(11):8014–29. https://doi.org/10.1016/j.ijhydene.2020.09.188.

[7] BHP. (2020). *BHP awards world's first LNG-fuelled Newcastlemax bulk carrier tender to reduce emissions*. https://www.bhp.com/media-and-insights/news/2020/09/bhp-awards-worlds-first-lng-fuelled-newcastlemax-bulk-carrier-tender-to-reduce-emissions/.

[8] BlueScope Steel. (2020). *XLERPLATE steel environmental product declaration* (S-P-00558 V2, Issue. https://epd-australasia.com/wp-content/uploads/2018/04/BSS22179-XLER_EPD_2020_Final.pdf.

[9] Chen C, Yang A. Power-to-methanol: the role of process flexibility in the integration of variable renewable energy into chemical production. Energy Convers Manage 2021;228:113673. https://doi.org/10.1016/j.enconman.2020.113673.

[10] COAG Energy Council. (2019). *Australia's national hydrogen strategy*. Commonwealth of Australia.

[11] Daehn KE, Cabrera Serrenho A, Allwood JM. How will copper contamination constrain future global steel recycling? Environ Sci Technol 2017;51(11):6599–606. https://doi.org/10.1021/acs.est.7b00997.

[12] Davis SJ, Lewis NS, Shaner M, Aggarwal S, Arent D, Azevedo IL, et al. Net-zero emissions energy systems. Science 2018;360(6396). https://doi.org/10.1126/science:aas9793.

[13] Deetman S, Marinova S, van der Voet E, van Vuuren DP, Edelenbosch O, Heijungs R. Modelling global material stocks and flows for residential and service sector buildings towards 2050. J Cleaner Prod 2020;245:118658. https://doi.org/10.1016/j.jclepro.2019.118658.

[14] Department of Industry, Science, Energy and Resources (DISER). (2020a). *Australian energy statistics, Table O: Australian electricity generation, by fuel type, physical units* Australian Government.

[15] Department of Industry, Science, Energy and Resources (DISER). (2020b). *Resources and energy quarterly: December 2020*. https://publications.industry.gov.au/publications/resourcesandenergyquarterlydecember2020/index.html.

[16] Department of Industry, Science, Energy and Resources (DISER). (2020c). *Technology investment roadmap: first low emissions technology statement – 2020*. https://www.industry.gov.au/sites/default/files/September%202020/document/first-low-emissions-technology-statement-2020.pdf.

[17] Fan Z, Friedmann SJ. Low-carbon production of iron and steel: technology options, economic assessment, and policy. Joule 2021;5(4):829–62. https://doi.org/10.1016/j.joule.2021.02.018.

[18] Gallo AB, Simões-Moreira JR, Costa HKM, Santos MM, Moutinho dos Santos E. Energy storage in the energy transition context: a technology review. Renew Sustain Energy Rev 2016;65:800–22. https://doi.org/10.1016/j.rser.2016.07.028.

[19] Geoscience Australia. (2021). *Hydrogen*. https://www.ga.gov.au/scientific-topics/energy/resources/hydrogen#heading-4.

[20] Giddey S, Badwal SPS, Munnings C, Dolan M. Ammonia as a renewable energy transportation media. ACS Sustainable Chem Eng 2017;5(11):10231–9. https://doi.org/10.1021/acssuschemeng.7b02219.

[21] Gielen D, Saygin D, Taibi E, Birat J. Renewables-based decarbonization and relocation of iron and steel making: a case study. J Ind Ecol 2020;24(5):1113–25. https://doi.org/10.1111/jiec.v24.510.1111/jiec.12997.

[22] Graham, P., Hayward, J., Foster, J., & Havas, L. (2020). *GenCost 2019-20*.

[23] Hadjipaschalis I, Poullikkas A, Efthimiou V. Overview of current and future energy storage technologies for electric power applications. Renew Sustain Energy Rev 2009;13(6):1513–22. https://doi.org/10.1016/j.rser.2008.09.028.

[24] Horvath, L. (2013). *Energy use in the steel industry*, IEAGHG/IETS Iron & Steel Industry CCUS and Process Integration Workshop, Tokyo, Japan. https://ieaghg.org/docs/General_Docs/Iron%20and%20Steel%202%20Secured%20presentations/1620%20Ladislav%20Horvath.pdf.

[25] Hosokai S, Kasiwaya Y, Matsui K, Okinaka N, Akiyama T. Ironmaking with ammonia at low temperature. Environ Sci Technol 2011;45(2):821–6. https://doi.org/10.1021/es102910q.

[26] Hot Briquetted Iron Association. (2009). *HBI Guide for handling, maritime carriage, and storage*. https://maritimecyprus.files.wordpress.com/2016/11/hbi-hot-briquetted-iron-guide-12-10-09.pdf.

[27] IEA. (2015). *Technology roadmap - hydrogen and fuel cells*. https://www.iea.org/reports/technology-roadmap-hydrogen-and-fuel-cells.

[28] IEA. (2019). *The future of hydrogen*. https://www.iea.org/reports/the-future-of-hydrogen.

[29] IEA. (2020). *Iron and steel technology roadmap* (Energy Technology Perspectives, Issue 15). https://www.iea.org/reports/iron-and-steel-technology-roadmap.

[30] IEA. (2021). *Net-zero by 2050: a roadmap for the global energy sector*. https://iea.blob.core.windows.net/assets/405543d2-054d-4cbd-9b89-d174831643a4/NetZeroby2050-ARoadmapfortheGlobalEnergySector_CORR.pdf.

[31] IEA Environmental Projects. (2013). *Iron and steel CCS study: techno-economics integrated steel mill*. International Energy Agency. http://documents.ieaghg.org/index.php/s/P3rYI5vSh80SPM7.
[32] IRENA. (2020). *Green hydrogen cost reduction: scaling up electrolysers to meet the 1.5℃ climate goal*. International Renewable Energy Agency, Abu Dhabi. https://irena.org/-/media/Files/IRENA/Agency/Publication/2020/Dec/IRENA_Green_hydrogen_cost_2020.pdf.
[33] Kim K, Roh G, Kim W, Chun K. A preliminary study on an alternative ship propulsion system fueled by ammonia: environmental and economic assessments. J Marine Sci Eng 2020;8(3):183. https://doi.org/10.3390/jmse8030183.
[34] Krüger, A., Andersson, J., Grönkvist, S., & Cornell, A. (2020). Integration of water electrolysis for fossil-free steel production. *Int J Hydrogen Energy*, *45*(55), 29966-29977. https://doi.org/10.1016/j.ijhydene.2020.08.116.
[35] Liberty Primary Steel. (2020). *Environmental product declaration: hot rolled structural and rail* (S-P-01547 Version 1, Issue. https://www.libertygfg.com/media/334834/2-epd_liberty-hot-rolled-structural-rail.pdf.
[36] Marcinkoski, J., Vijayagopal, R., Adams, J., James, B., Kopasz, J., & Ahluwalia, R. (2019). *DOE advanced truck technologies*. https://www.hydrogen.energy.gov/pdfs/19006_hydrogen_class8_long_haul_truck_targets.pdf.
[37] McFarlane, D. (2015). *Water resource assessment for the Pilbara*.
[38] McKinlay CJ, Turnock S, Hudson D. *A comparison of hydrogen and ammonia for future long distance shipping fuels*. LNG/LPG and Alternative Fuel Ships. London: Royal Institute of Naval Architects; 2020. https://eprints.soton.ac.uk/437555/.
[39] Mekhilef S, Saidur R, Safari A. Comparative study of different fuel cell technologies. Renew Sustain Energy Rev 2012;16(1):981–9. https://doi.org/10.1016/j.rser.2011.09.020.
[40] Ministry of Land, Infrastructure, Transport and Tourism. (2007). *Land and climate of Japan*. Government of Japan.
[41] Mission Possible Partnership. (2021). *Steeling demand: mobilising buyers to bring net-zero steel to market before 2030*. https://www.energy-transitions.org/wp-content/uploads/2021/07/2021-ETC-Steel-demand-Report-Final.pdf.
[42] Müller N, Herz G, Reichelt E, Jahn M, Michaelis A. Assessment of fossil-free steelmaking based on direct reduction applying high-temperature electrolysis. Cleaner Eng Technol 2021;4:100158. https://doi.org/10.1016/j.clet.2021.100158.
[43] Nayak-Luke R, Bañares-Alcántara R, Wilkinson I. "Green" ammonia: impact of renewable energy intermittency on plant sizing and levelized cost of ammonia. Ind Eng Chem Res 2018;57(43):14607–16. https://doi.org/10.1021/acs.iecr.8b02447.
[44] Peters R, Deja R, Engelbracht M, Frank M, Nguyen VN, Blum L. Efficiency analysis of a hydrogen-fueled solid oxide fuel cell system with anode off-gas recirculation. J Power Sources 2016;328:105–13. https://doi.org/10.1016/j.jpowsour.2016.08.002.
[45] Pilbara Development Commission. *Our region*. Government of Western Australia. Retrieved September 21, 2021, from https://www.pdc.wa.gov.au/our-region/region-pilbara.
[46] Pilbara Ports Authority. (2020). *2020 port handbook*. https://www.pilbaraports.com.au/about-ppa/publications/forms-and-publications/forms-publications/handbook/2020/june/port-of-port-hedland-2020-handbook-high-quality.
[47] Pimm AJ, Cockerill TT, Gale WF. Energy system requirements of fossil-free steelmaking using hydrogen direct reduction. J Cleaner Prod 2021;312:127665. https://doi.org/10.1016/j.jclepro.2021.127665.
[48] Reserve Bank of Australia. (2021). *Inflation calculator*. https://www.rba.gov.au/calculator/annualDecimal.html.
[49] Rubio D, Casanueva JF, Nebot E. Assessment of the antifouling effect of five different treatment strategies on a seawater cooling system. Appl Therm Eng 2015;85:124–34. https://doi.org/10.1016/j.applthermaleng.2015.03.080.
[50] S&P Global Platts. (2021). *PortWorld: distance calculator*. https://www.portworld.com/map.
[51] Scataglini, R., Mayyas, A., Wei, M., Chan, S. H., Lipman, T., Gosselin, D., D'Alessio, A., Breunig, H., Colella, W. G., & James, B. D. (2015). *A total cost of ownership model for solid oxide fuel cells in combined heat and power and power only applications*. https://www.energy.gov/eere/fuelcells/downloads/total-cost-ownership-model-solid-oxide-fuel-cells-combined-heat-and-power.
[52] Schlosser CA, Strzepek K, Gao X, Fant C, Blanc É, Paltsev S, et al. The future of global water stress: an integrated assessment. Earth's Future 2014;2(8):341–61. https://doi.org/10.1002/2014EF000238.
[53] Speirs J, McGlade C, Slade R. Uncertainty in the availability of natural resources: fossil fuels, critical metals and biomass. Energy Policy 2015;87:654–64. https://doi.org/10.1016/j.enpol.2015.02.031.
[54] Steelonthenet.com. (2021). *Semi-finished steel prices*. https://www.steelonthenet.com/semi-finished-prices.php.
[55] Stolzenburg, K., Berstad, D., Decker, L., Elliott, A., Haberstroh, C., Hatto, C., Klaus, M., Mortimer, N., Mubbala, R., & Mwabonje, O. (2013). *Efficient liquefaction of hydrogen: results of the IDEALHY project* XXth energie – symposium, Stralsund/Germany.
[56] Talens Peiró L, Villalba Méndez G. Material and energy requirement for rare earth production. JOM 2013;65(10):1327–40. https://doi.org/10.1007/s11837-013-0719-8.
[57] The Climate Group. (2021). *SteelZero*. https://www.theclimategroup.org/steelzero.
[58] Thyssenkrupp. (2018). *Hydrogen from large-scale electrolysis*. https://ucpcdn.thyssenkrupp.com/_binary/UCPthyssenkruppBAISUhdeChlorineEngineers/en/products/water-electrolysis-hydrogen-production/power-to-gas/link-thyssenkrupp_Hydrogen_Water_Electrolysis_and_green_chemicals.pdf.
[59] Tong W, Forster M, Dionigi F, Dresp S, Sadeghi Erami R, Strasser P, et al. Electrolysis of low-grade and saline surface water. Nat Energy 2020;5(5):367–77. https://doi.org/10.1038/s41560-020-0550-8.
[60] Tronstad, T., Astrand, H. H., Haugom, G. P., & Langfeldt, L. (2017). *Study on the use of fuel cells in shipping*. EMSA European Maritime Safety Agency.
[61] UNCTAD. (2020). *Review of maritime transport*. https://unctad.org/system/files/official-document/rmt2020_en.pdf.
[62] Vecteezy.com. (2021). World map free vector.
[63] Vogl, V., Åhman, M., & Nilsson, L. J. (2018). Assessment of hydrogen direct reduction for fossil-free steelmaking. *J Clean Product*, *203*, 736-745. https://doi.org/10.1016/j.jclepro.2018.08.279.
[64] Water Technology. (2021). *Perth seawater desalination plant*. Retrieved 19/07/2021 from https://www.water-technology.net/projects/perth/.
[65] Whiston MM, Azevedo IML, Litster S, Samaras C, Whitefoot KS, Whitacre JF. Meeting U.S. solid oxide fuel cell targets. Joule 2019;3(9):2060–5. https://doi.org/10.1016/j.joule.2019.07.018.
[66] Wijayanta AT, Oda T, Purnomo CW, Kashiwagi T, Aziz M. Liquid hydrogen, methylcyclohexane, and ammonia as potential hydrogen storage: comparison review. Int J Hydrogen Energy 2019;44(29):15026–44. https://doi.org/10.1016/j.ijhydene.2019.04.112.
[67] Wood, T., Dundas, G., & Ha, J. (2020). *Start with steel*. Grattan Institute. https://grattan.edu.au/wp-content/uploads/2020/05/2020-06-Start-with-steel.pdf.
[68] World Steel Association. (2020a). Steel statistical yearbook.
[69] World Steel Association. (2020b). *Water management in the steel industry*. https://www.worldsteel.org/publications/position-papers/water-management.html.
[70] Wong JB, Zhang Q. Impact of carbon tax on electricity prices and behaviour. Finance Res Lett 2021;102098. https://doi.org/10.1016/j.frl.2021.102098.
[71] Foumani M, Smith-Miles K. The impact of various carbon reduction policies on green flowshop scheduling. Appl Energy 2019;249:300–15. https://doi.org/10.1016/j.apenergy.2019.04.155.